John D. Heit* and Shad Roundy

A Framework to Determine the Upper Bound on Extractable Power as a Function of Input Vibration Parameters

Abstract: This paper outlines a mathematical framework to determine the upper bound on extractable power as a function of the forcing vibrations. In addition, the method described provides insight into the dynamic transducer forces required to attain the upper bound. The relationship between vibration parameters and transducer force gives a critical first step in determining the optimal transducer architecture for a given vibration source. The method developed is applied to three specific vibration inputs: a single sinusoid, the sum of two sinusoids, and a single sinusoid with a time-dependent frequency. As expected, for the single sinusoidal case, the optimal transducer force is found to be that produced by a resonant linear spring and a viscous damping force, with matched impedance to the mechanical damper. The resulting transducer force for the input described by a sum of two sinusoids is found to be inherently time dependent. The upper bound on power output is shown to be twice that obtainable from a linear harvester centered at the lower of the two frequencies. Finally, the optimal transducer force for a sinusoidal input with a time-dependent frequency is characterized by a viscous damping term and a linear spring with a time-dependent coefficient.

Keywords: vibration energy harvesting, optimization, transducer dynamics

1 Introduction

Much recent work in vibration energy harvesting has focused on structure and transducer designs to improve power output from vibration sources that are not modeled as a single sinusoidal input. Much of this work has investigated the use of nonlinearities as a way to increase energy output (Roundy et al. 2005; Erturk, Hoffmann, and Inman 2009; Mann, Barton, and Owens 2012; Daqaq, 2012; Nguyen, Halvorsen, and Paprotny 2013; Daqaq et al. 2014). These nonlinearities are usually of the form of a nonlinear spring, such as a Duffing oscillator. For example, Hoffmann et al. (2012) showed that for certain vibration inputs a nonlinear mono-stable or bi-stable oscillator could provide 300% to 500% more power output compared to a linear system. However, this work had to assume a form for the restoring force before the parameters could be optimized for power generation. Such works give useful insight into the potential uses of nonlinearities for harvesting from complex vibration inputs. However, these works do not give a clear relationship between the parameters that define the input vibration and the optimal transducer dynamics.

Other researchers have taken the opposite approach, starting with the vibration excitation and investigating the optimal transducer architectures to extract the maximum power. Daqaq (2010, 2011) showed that for a two-state system excited by Gaussian white noise the energy generation was not a function of the transducer's potential function. That is to say that the restoring force of the system does not affect the power generation for a Gaussian white noise vibration input. This is true for a two-state system (i.e., the electrical states are not explicitly modeled) or when the ratio of mechanical to electrical time constants is small. In the same study, Daqaq examined the case for filtered white noise, where some frequencies are more represented than others. In this case he was forced to assume a form for the potential function in order to estimate a solution. In further studies, Daqaq (2012) showed that under certain conditions a bi-stable restoring force can outperform a standard linear oscillator-based vibration energy harvester when excited by Gaussian white noise. This is true when the mechanical to electrical time constant ratio is small and when the bi-stable potential function is designed based on the known intensity of the excitation. Halvorsen (2008, 2013) has also studied the effect of the electrical time constant on systems excited by Gaussian noise for both linear and

*Corresponding author: John D. Heit, Los Alamos National Laboratory, Los Alamos, NM 87545, USA, E-mail: heit88@gmail.com
Shad Roundy, Department of Mechanical Engineering, University of Utah, Salt Lake City, UT 84112, USA, E-mail: shad.roundy@utah.edu

nonlinear potential functions. His results support the general conclusions that under Gaussian white noise excitation, nonlinearities in the restoring force are beneficial only in specific circumstances, but are not uniformly beneficial.

Halvorsen et al. (2013) proved that for an input described by a single frequency harmonic (i.e., a single sinusoid) when the proof mass is subjected to viscous damping, the optimal transducer dynamics are those of a velocity-damped resonant generator (VDRG; Mitcheson et al. 2004). While Halvorsen et al. (2013) only applied their methodology to a single frequency input, their method could be profitably applied to a wider range of inputs that represent classes of real world vibrations. This work uses essentially the same method as Halvorsen et al., but applies it to two additional test cases. The method both finds the unconstrained globally optimal relationship between the input vibration and the force that must be produced by the transducer, and the upper limit for extractable power from a given vibration source. We do not explicitly constrain the dynamics of the energy harvester, but seek to find the optimal power output for any type of harvester. The remainder of this paper is organized as follows. First, the general model and equations for the optimal transducer force and power output are developed and applied to a vibration input characterized by a single stationary frequency. This section can be seen as a review of the method published by Halvorsen et al. (2013). The procedure is then applied to a vibration input characterized by two separate, but stationary, frequencies (i.e., the sum of two sinusoids). The final test case is a vibration input characterized by a time-dependent frequency. These two additional test cases illustrate the way in which the methodology can be used on more complex vibration sources.

2 Modeling

A simple, generic model for an inertial energy harvester, as shown in Figure 1, is a kinetic harvester with a generic transducer force F_T that acts on the proof mass. This generic transducer may contain both energy-dissipative elements for power generation and energy-conservative restoring elements. In general, the system is subject to a forcing function $F(t)$. The inherent mechanical losses that are found in any real system are approximated by a linear viscous damper described by a single coefficient b_m. This single-degree-of-freedom system is characterized by a single displacement x. If the system is excited through base excitation, as is the normal case for an inertial generator, then $F(t)$ would be the mass (m) multiplied
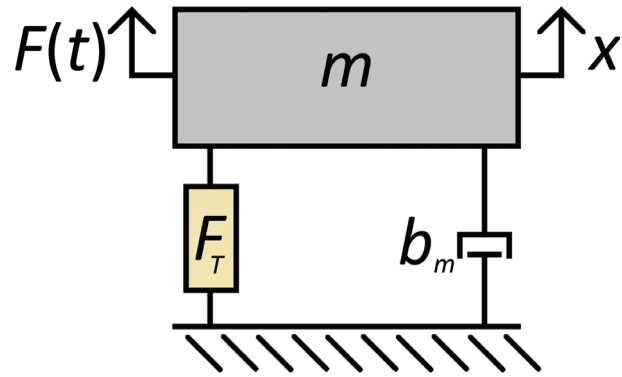

Figure 1: A generic inertial generator characterized by a relative displacement x. Here F_T represents the force produced by an unknown transducer architecture. b_m is the coefficient that characterizes the system's linear viscous damping due to inherent mechanical losses of the system.

by the base acceleration $A(t)$. In this case the displacement x is the relative distance between the proof mass and ground. This system is modeled by eq. [1]:

$$m\ddot{x} + b_m\dot{x} + F_T = F(t) \qquad [1]$$

The second-order differential equation [1] that models this generic system can be expressed in state space form by letting $x_1 = x$, and $x_2 = \dot{x}$:

$$\dot{x}_1 = x_2 \qquad [2]$$

$$\dot{x}_2 = \frac{1}{m}\left(-b_m x_2 - F_T + F(t)\right) \qquad [3]$$

An energy balance of the system is used in order to find an expression for the energy generated by the transducer as a function of the input. By examining the energy balance of the system in steady state we can neglect the kinetic energy of the mass as well as the possible potential energy stored in the transducer. This is due to the fact that these energy storage elements are restorative, thus they do not represent a net energy input or output to the system while it is in steady state. The energy balance equations are

$$E_{in} = E_{out} \qquad [4]$$

$$E_{in} = \int F(t)x_2 dt \qquad [5]$$

$$E_{out} = \int b_m x_2^2 dt + E_{gen} \qquad [6]$$

Substituting eqs [5] and [6] into eq. [4] will yield an expression for the energy generated as a function of the input force and the velocity of the proof mass.

$$E_{\text{gen}} = \int \left[F(t)x_2 - b_m x_2^2 \right] dt \qquad [7]$$

For more generalized results we can look at the square of the power to examine a continuous positive definite functional, thereby allowing us to find the critical points in the magnitude of the energy generated:

$$J = \int \left[F(t)x_2 - b_m x_2^2 \right]^2 dt \qquad [8]$$

Equation [8] now represents the time integral of the square of the instantaneous power generated by the transducer. The introduction of J allows for the examination of a positive definite functional. By examining the critical points of this functional, as opposed to the instantaneous power, a third solution is realized, over the two available from looking at the integrand of eq. [7]. As will become apparent below, this third solution is a minimum which results in zero energy generation. However, it is instructive to investigate all stationary conditions, and therefore we have chosen to use the functional J instead of the instantaneous power generated. If the velocity of the proof mass x_2 is treated as the control parameter, the critical points of the functional can be found through the stationary condition of the Euler–Lagrange equation (Bryson, 1975). Taking I to be the integrand of eq. [8] we have

$$I = \left[F(t)x_2 - b_m x_2^2 \right]^2 = F(t)^2 x_2^2 - 2b_m F(t)x_2^3 + b_m^2 x_2^4 \qquad [9]$$

and the stationary condition to be

$$\frac{dI}{dx_2} = 0 \qquad [10]$$

In this case the stationary condition yields the critical points of the energy generated with respect to the velocity path of the proof mass. Equation [3] can be used to relate the velocity of the proof mass and the force of the transducer, F_T, acting on the proof mass. This relationship will allow an expression for the necessary transducer force such that the proof mass will follow the calculated optimal velocity path for energy generation. Solving the stationary condition for the critical velocities of x_2

$$\frac{dI}{dx_2} = 2F(t)^2 x_2 - 6b_m F(t)x_2^2 + 4b_m^2 x_2^3 = 0 \qquad [11]$$

$$(F(t) - 2b_m x_2)(F(t) - b_m x_2)x_2 = 0 \qquad [12]$$

By factorization, the resulting three solutions are apparent. Here $\star$ denotes a critical path with respect to the energy generated.

$$x_2^\star = \frac{F(t)}{2b_m} \qquad [13]$$

$$x_2^\star = \frac{F(t)}{b_m} \qquad [14]$$

$$x_2^\star = 0 \qquad [15]$$

These three relationships for $x_2^\star$ represent the critical velocity paths which, given a vibration input $F(t)$ to the system, will result in a minimum or maximum energy output. By substituting these signals into the second derivative the type of critical points are determined. The second derivative is found to be

$$\frac{d^2 I}{dx^2} = 2F(t)^2 - 12b_m F(t)x_2 + 12b_m^2 x_2^2 \qquad [16]$$

At $x_2^\star = \frac{F(t)}{2b_m}$:

$$\frac{d^2 I}{dx^2} = 2F(t)^2 - 6F(t)^2 + 3F(t)^2 = -F(t)^2 \qquad [17]$$

which is negative for all input vibrations $F(t)$.
At $x_2^\star = \frac{F(t)}{b_m}$:

$$\frac{d^2 I}{dx^2} = 2F(t)^2 - 12F(t)^2 + 12F(t)^2 = 2F(t)^2 \qquad [18]$$

which is positive for all input vibrations $F(t)$.
At $x_2^\star = 0$:

$$\frac{d^2 I}{dx^2} = 2F(t)^2 \qquad [19]$$

which is positive for all input vibrations $F(t)$.

From this examination we can conclude that $x_2^\star = \frac{F(t)}{2b_m}$ corresponds to the maximum energy generated by the transducer for a given input force, while $x_2^\star = \frac{F(t)}{b_m}$ and $x_2^\star = 0$ correspond to a minimum amount of energy generated.

By substituting these relationships into the governing differential equations [2–3], an expression for the displacement of the proof mass x_1 as well as the transducer force F_T can be expressed as a function of the system properties and the input force.
For $x_2^\star = \frac{F(t)}{2b_m}$:

$$x_1^\star = \int \frac{F(t)}{2b_m} dt \qquad [20]$$

$$F_T^\star = -\frac{m\dot{F}(t)}{2b_m} + \frac{F(t)}{2} \qquad [21]$$

Similarly for $x_2^\star = \frac{F(t)}{b_m}$:

$$x_1^\star = \int \frac{F(t)}{b_m} dt \qquad [22]$$

$$F_T^\star = \frac{-m\dot{F}(t)}{b_m} \qquad [23]$$

Table 1: Summary of critical path relationships for a generic input.

Critical velocity path	Critical position path	Critical transducer force	Type
$x_2^\star = \frac{F(t)}{2b_m}$	$x_1^\star = \int \frac{F(t)}{2b_m}\,dt$	$F_T^\star = -\frac{m\dot{F}(t)}{2b_m} + \frac{F(t)}{2}$	Maximum
$x_2^\star = \frac{F(t)}{b_m}$	$x_1^\star = \int \frac{F(t)}{b_m}\,dt$	$F_T^\star = -\frac{m\dot{F}(t)}{b_m}$	Minimum
$x_2^\star = 0$	$x_1^\star = 0$	$F_T^\star = F(t)$	Minimum

And for $x_2^\star = 0$

$$x_1^\star = 0 \tag{24}$$

$$F_T^\star = F(t) \tag{25}$$

Here, the transducer force, F_T, is an explicit function of time. The optimal transducer can only then be represented as a function of states if the input and its derivative can be expressed as a function of the states through the corresponding relationships of x_1 and x_2. These results are summarized in Table 1. Equations [24] and [25] correspond to the trivial solution of a stationary condition of the proof mass.

3 Case Study Results

It is difficult to see the relevance of eqs [20–23] in their general form. To help illustrate the utility of these relationships, three types of vibration inputs were analyzed: a single sinusoid (i.e., single stationary frequency), a sum of two sinusoids (i.e., two stationary frequencies), and a sinusoid with a time-dependent frequency (i.e., a sine sweep).

3.1 Single Sinusoid Input

First we will look at the relationship that maximizes the energy output of the system, and then examine the conditions that create minimum energy output. For the maximum power condition $x_2^\star = \frac{F(t)}{2b_m}$, letting $F(t) = A\,m\sin(\omega t)$ results in the following relationships:

$$x_1^\star = -\frac{Am}{2b_m\omega}\cos(\omega t) \tag{26}$$

$$x_2^\star = \frac{Am}{2b_m}\sin(\omega t) \tag{27}$$

$$F_T^\star = -\frac{A\omega m^2}{2b_m}\cos(\omega t) + \frac{Am}{2}\sin(\omega t) \tag{28}$$

Substituting for $x_1^\star$ and $x_2^\star$:

$$F_T^\star = \omega^2 m x_1 + b_m x_2 \tag{29}$$

Similarly for the minimum energy case in which $x_2^\star = \frac{Am}{b_m}\sin(\omega t)$:

$$F_T^\star = \omega^2 m x_1 \tag{30}$$

And for $x_2^\star = 0$:

$$F_T^\star = F(t) \tag{31}$$

The three results for the critical transduction force can be interpreted as follows: for the maximizing condition, $x_2^\star = \frac{F(t)}{2b_m}$, the optimal transducer model is a linear spring and a linear viscous damper for an electrical transducer. The constant of the linear spring is found to be resonant with the vibration input and the impedance of the electrical damper is found to be matched to the impedance of the mechanical damper. That is, b_m, from eqs [1] and [3], is the same value as b_m for the transducer in eq. [29]. This system is a completely passive system, being only a function of the system's states. The system is shown in Figure 2 and modeled by the differential equation [32].

$$m\ddot{x} + 2b_m\dot{x} + kx = F(t) \tag{32}$$

If the form of the transducer force is assumed to be a linear viscous damper in parallel with a linear spring, the
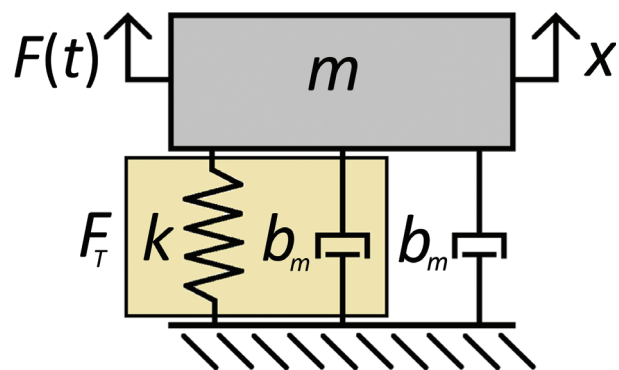

Figure 2: Optimal power transducer architecture for an input $F(t) = A\,m\sin(\omega t)$, where $k = \omega^2 m$.

coefficients that result in maximum power generation are widely known and have been previously reported (Roundy, Wright, and Rabaey 2003; Mitcheson et al. 2004; Halvorsen et al. 2013). This framework yielded the known optimal transducer, without any assumptions on the form of the transducer. By using this simple vibration input, with a known solution, this mathematical framework was able to be verified.

For the critical path $x_2^\star = \frac{Am}{b_m}\sin(\omega t)$, which corresponds to a minimum power condition the corresponding transducer force is a linear spring with spring constant $k = \omega^2 m$. This system is shown in Figure 3 and modeled by eq. [33]. While this system has a large response in x_1 to the input $F(t) = A m \sin(\omega t)$, no energy will be converted to useful electric energy since the system's only dissipative element is from parasitic losses due to mechanical damping. The final relationship $x_2^\star = 0$ gives the trivial stationary solution for the energy output, as previously mentioned. Under this condition, the transducer force F_T provides an equal and opposite force to the input $F(t)$ on the mass in order to keep the proof mass stationary. In the case of base excitation, the relative displacement between the proof mass and ground is zero. Physically this would be accomplished by the use of an infinitely stiff spring for the transducer, $k = \infty$.

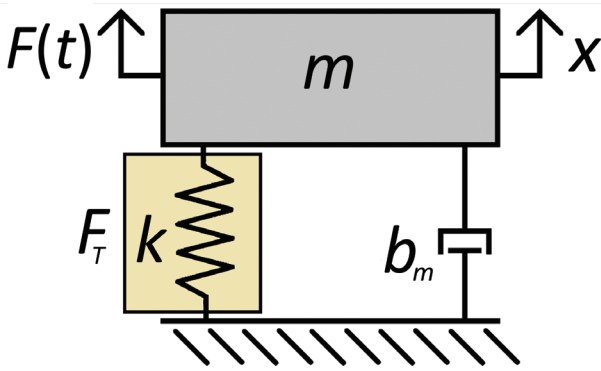$$m\ddot{x} + b_m\dot{x} + kx = F(t) \qquad [33]$$

Figure 3: Transduction model for the minimum energy output: $x_2^\star = \frac{F(t)}{b_m}$ ($k = \omega^2 m$) and $x_2^\star = 0$ ($k = \infty$).

3.2 Double Sinusoid Input

A common vibration input is one of two simultaneous sinusoids at different frequencies. This type of vibration occurs in rotating machinery where two unbalanced masses rotate at different rates fixed relative to one another or in a system where multiple harmonics are well represented.

The root mean square (RMS) power output scales with A^2 for the standard linear system. Thus, the case where the amplitudes of the two sinusoids are equal will be examined. In the case where one sinusoid has an amplitude much greater than the other, it is reasonable to assume that the maximum power generation will be achieved by creating a linear harvester tuned to the frequency corresponding to the maximum value of $\frac{A^2}{\omega}$. In the case where the two sinusoids are of similar, but different amplitudes, the following analysis is relevant. The expression for this double sinusoidal input is shown in eq. [34].

$$F(t) = Am(\sin(\omega t) + \sin(n\omega t)) \qquad [34]$$

Here, $n \in (0\ \infty)$ represents the multiple difference between the two frequency components.

Examining now only the input-velocity relationship from eq. [13], which results in the maximum energy output, the optimal velocity signal for an input of two sinusoids is obtained as

$$x_2^\star = \frac{Am}{2b_m}(\sin(\omega t) + \sin(n\omega t)) \qquad [35]$$

Using eqs [20] and [21] the relationships for the optimal position path and corresponding transducer force to achieve the velocity response as shown in eq. [35] can be written as

$$x_1^\star = -\frac{Am}{2\omega b_m}\left(\cos(\omega t) + \frac{1}{n}\cos(n\omega t)\right) \qquad [36]$$

$$F_T^\star = \frac{Am}{2}(\sin(\omega t) + \sin(n\omega t)) - \frac{A\omega m^2}{2b_m}(\cos(\omega t) + n\cos(n\omega t)) \qquad [37]$$

Substituting eqs [36] and [35] for x_1 and x_2 into eq. [37], where available, yields

$$F_T^\star = b_m x_2 + \omega^2 m x_1 + TD \qquad [38]$$

where TD is the time-dependent component of the transducer force that cannot be directly substituted for by the system states x_1 and x_2.

$$TD = \frac{A\omega m^2}{2b_m}\left(\frac{1}{n} - n\right)\cos(n\omega t) \qquad [39]$$

From eq. [39] it can be seen that when there is only one frequency component, when $n = 1$, the amplitude of the time-dependent portion of the transducer is zero. This intuitive result for the transducer force shows that as $n \to 1$ the amplitude of the time-dependent component goes to zero and the transducer architecture converges to the linear harvester as seen for the single sinusoidal

input in eq. [29]. However, as $n \to 0$ or ∞ the amplitude of the time-dependent portion of the transducer force grows without bound, as is shown in Figure 4.
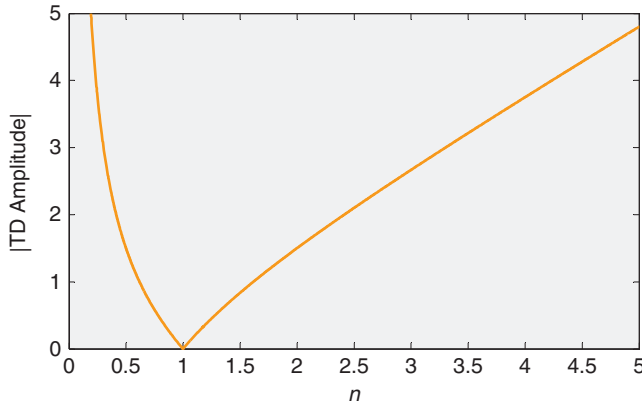

Figure 4: The effect of n on the amplitude of the time-dependent component of the transducer force.

The time-dependent component of the transducer force shows that the true unconstrained optimal transducer force for an input vibration of this form cannot be realized by a passive system that is a function of the two states of the system shown in Figure 1. The optimal force requires that the transducer introduce new states to the system or be implemented with active structures that do work on the system. An example of the optimal restoring force is shown in Figure 5.

An analysis of a transducer that introduces additional states is outside the scope of the present study. The desire here is to simply determine the upper bound on power generation. To determine this true upper bound, we need to determine whether the time-dependent force does work adding energy to the system over time, takes energy from the system, or does no net work on the system and acts as a conservative element. The net energy into the proof mass from the time-dependent force can be calculated by integrating the force over the displacement for a period T of the entire signal:

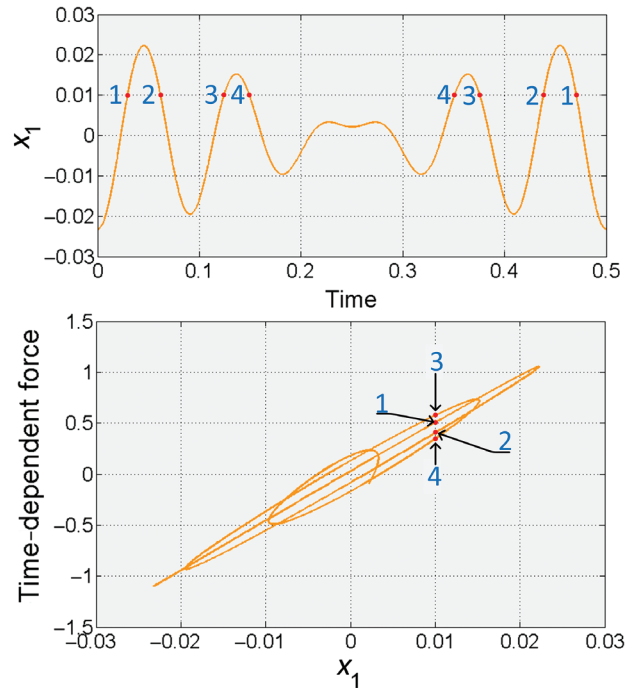$$E_{TD} = \int_0^T TD dx_1 = \int_0^T TD * x_2^* dt \qquad [40]$$

Figure 5: (Top) The steady-state position of the proof mass versus time for $n = 1.2$. This complex path repeats itself every period T of the input signal. (Bottom) The time-dependent force plotted over the optimal path x_1 over a period T. It can be seen that during one period the same position is repeated multiple times, but requires a different transducer force.

Substituting eqs [39] and [35] for the time-dependent portion of the transducer and optimal velocity path, respectively.

$$E_{TD}(t) = \frac{A^2 \omega m^3}{4b_m^2}\left(\frac{1}{n} - n\right) * \int_0^T (\sin(\omega t)\cos(n\omega t) \\ + \sin(n\omega t)\cos(n\omega t))dt \qquad [41]$$

where T is the complete period of the input vibration. This period can be found by finding the point in time in which the periods of the two sinusoidal components simultaneously occur. This can be found by finding the integer value κ such that $\kappa * n \in Z^+$. The total period for any input of this form is then defined by $T = \frac{2\pi}{\omega}\kappa$.

Evaluating eq. [41]:

$$E_{TD}\left(\frac{2\pi}{\omega}\kappa\right) = \frac{A^2 m^3\left(1 - (-2+n)n - n(1+n)\text{Cos}[2\kappa(-1+n)\pi] + (-1+n^2)\cos(2\kappa n\pi)^2 + (-1+n)n\cos(2\kappa(1+n)\pi)\right)}{8b^2 n^2}$$

$$[42]$$

For the constraints of $\kappa \in Z$ and $n * \kappa \in Z$ eq. [42] reduces to zero. This shows that the time-dependent force acts as a conservative element, not doing any work to the system over time.

The upper limit for energy output from the optimal transducer can be shown analytically. This can be accomplished in a similar manner to the derivation of the average power output for the single sinusoid case. Knowing that from the result of eq. [38] the power output from the transducer is dissipated by the force of a linear viscous damper, the instantaneous power dissipated through this element can be written as

$$P = F * v = b_m x_2^{\star 2} \qquad [43]$$

Here $x_2^\star$ is the optimal velocity shown in eq. [35]. Integrating the instantaneous power output over time yields the total energy generated by the transducer. Again the upper limit of the integral is defined as the period of the input.

$$E_n = \int_0^{\frac{2\pi \kappa}{\omega}} b_m x_2^{\star 2} dt \qquad [44]$$

The integral is then evaluated in the general case for all $n \in (1, \infty)$.

$$E_n = \frac{A^2 m^2 T}{4 b_m} \qquad [45]$$

Note that for all $n \neq 1$, the rms value of the excitation force is Am. However, for the special case in which $n = 1$, the rms value of the excitation force is $\sqrt{2}\, Am$, and thus the upper bound on the energy generated would be double that shown in eq. [45]. However, if the rms value of the driving force is normalized to Am for the special case of $n = 1$, eq. [45] will still hold. The result is that the upper bound on power output is not a function of n. Intuitively this means that if the transducer force given by eqs [38] and [39] can be generated, all of the power from both sinusoids could, in theory, be captured.

In order to gain additional insight into eq. [45] a numerical study was performed in which the energy output over a sufficiently long period was measured for various values of n. The output of this study is shown in Figure 6. In one case, the optimal transducer force is applied to the proof mass. In the second case, the system is characterized by a linear oscillator whose resonance is the lower of the two frequencies present in the forcing vibrations. The output is normalized to the energy generated by either system at $n = 1$. As n deviates from 1, the power output from the linear system quickly drops to ½. However, the power output from the optimal system remains constant at 1.

We pause here to reiterate that the results obtained are specific to a two-state system, position (x_1) and velocity (x_2) in this case. (In other words, the transducer does not add states to the system.) Of course, it is possible to add states to the system by introducing additional energy storage elements as part of the transducer in either the mechanical or electric domain. If additional states are introduced, the same results as shown in Figure 6 could be obtained through complex conjugate matching for the two frequencies that are represented in the forcing function. In fact, if the forcing function is well represented by a set of stable, discrete frequencies, a complex conjugate matching network could be used to extract the power from each of the frequencies. However, if the forcing function contains a continuous band of frequencies, the complex conjugate matching method will not work. Such a situation is explored in the third case study below.
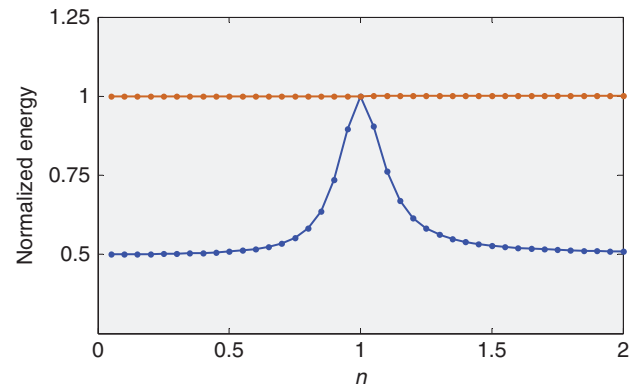

Figure 6: Numeric simulations of the energy output of the optimal transducer (orange) as compared to a linear harvester (blue) as a function of n, the separation between the two sinusoids in the forcing function. The energy produced by the optimal transducer (top line) is independent of n. The energy production has been normalized by the energy output of both systems at $n = 1$.

The time-dependent force given in eq. [39] is conservative. It could be implemented, for example, by a transducer that adds states to the system. Adding states to the system necessarily takes space (e.g., sprung mass, inductance) or power (e.g., synthesized impedances). It is a question for a specific system implementation to determine if the addition of the elements to produce the time-dependent force is more beneficial than simply adding extra sprung mass that oscillates at the lower of the two frequencies represented in the forcing function. In any case, such an analysis is outside the scope of this paper. Our primary goal is to demonstrate a method to determine the maximum extractable power.

3.3 Swept Sinusoid Input

Another common vibration input is one of a single sinusoid with a time-dependent frequency. A common occurrence of this input type is found in a variety of transportation applications. These applications range from the quickly varying rotational speed of an automobile tire, as experienced by a tire pressure monitor, to the slow changing excitation experienced by trains. Machinery with an unbalanced mass, whose rotational speed is time dependent, also experiences this type of excitation. Another occurrence of this input is in structural health monitoring. In this application the fundamental frequency of the structure changes very slowly with ambient conditions such as temperature.

Using the relationship from eq. [13], corresponding to the maximum power output, the optimal velocity path as a function of the vibration input is described by

$$x_2^\star = \frac{Am}{2b_m} \mathrm{Sin}\left[2\pi\left(f_0 + \frac{1}{2}f_r t\right)t\right] \qquad [46]$$

Equation [3] can be used to find the relationship for the optimal transducer force and is shown in eq. [47]. However, in this case eq. [2] cannot be used to solve for the optimal position path of the proof mass x_1 as an analytical solution to the integral of $x_2^\star$ can only be expressed through the use of Fresnel integrals. This relationship does not allow for a direct substitution of a function of x_1 for the optimal transducer force:

$$\begin{aligned} F_T^\star = &\frac{Am}{2} \mathrm{Sin}\left[2\pi\left(f_0 + \frac{1}{2}f_r t\right)t\right] \\ &- \frac{\pi Am^2}{b_m}(f_0 + f_r t)\mathrm{Cos}\left[2\pi\left(f_0 + \frac{1}{2}f_r t\right)t\right] \end{aligned} \qquad [47]$$

The same substitution as for the single and double sinusoid can be made for the first term of eq. [47] by a linear viscous damper model with matched impedance to the mechanical damping:

$$F_T^\star = b_m x_2 + TD \qquad [48]$$

Here, TD is again the time-dependent portion of the transducer force that cannot be substituted directly by the states of the system:

$$TD = -\frac{\pi Am^2}{b_m}(f_0 + f_r t)\mathrm{Cos}\left[2\pi\left(f_0 + \frac{1}{2}f_r t\right)t\right] \qquad [49]$$

With the single sinusoid case in mind, the mathematical framework can be used to check the validity of an assumed optimal transducer. Specifically, the optimal transducer is assumed to be a linear spring with a time-dependent stiffness coefficient that maintains resonance

with the input frequency at all times. Since the viscous damping which represents energy generation is already expressed in eq. [48], the missing component of the assumed transducer is this time-varying spring component. It is assumed that the time-dependent portion of the transducer force, given in eq. [49], is this time-dependent spring. Mathematically, this assumption is expressed as

$$TD = k(t)x_1 = \omega(t)^2 m x_1 = (2\pi(f_0 + f_r t))^2 m x_1 \qquad [50]$$

This relationship can be used to find an expression for x_1 that can subsequently be differentiated for x_2. To validate the accuracy of our assumption in eq. [50], x_2 from the assumed optimal transducer architecture will be compared to $x_2^\star$ in eq. [46].

Substituting eq. [49] into eq. [50] and solving for x_1 yields

$$x_1 = -\frac{Am}{4\pi b_m(f_0 + f_r t)}\mathrm{Cos}\left[2\pi\left(f_0 + \frac{1}{2}f_r t\right)t\right] \qquad [51]$$

By differentiation the velocity path of the assumed optimal transducer x_2 is found to be

$$\begin{aligned} x_2 = &\frac{Amf_r}{4\pi b_m(f_0 + f_r t)^2}\mathrm{Cos}\left[2\pi\left(f_0 + \frac{1}{2}f_r t\right)t\right] \\ &+ \frac{Am}{2b_m}\mathrm{Sin}\left[2\pi\left(f_0 + \frac{1}{2}f_r t\right)t\right] \end{aligned} \qquad [52]$$

Examining the two components of eq. [52] we can see that the second term is identical to the expression of $x_2^\star$ in eq. [46]. The first term of the expression is a transient sinusoid with decaying amplitude. An example comparison between x_2 and $x_2^\star$ is shown in Figure 7 with unitary values of the parameters and a relatively large value for f_r of 10Hz/sec.

The transient component that causes the incongruity between x_2 and $x_2^\star$ is only appreciable for large values of f_r over small time scales relative to the initial period $\frac{1}{f_0}$. In application, the value of f_r will generally be fairly small as any structure will require an input of energy to adjust the resonance frequency of the system.

Through this example we have shown that the mathematical framework can be used to validate an assumed optimal architecture. This framework can be used as a basis of comparison between transducer architectures and as a mark of feasibility for implementing a vibration energy harvester for a given vibration input and power requirement.

The upper limit for the energy output of the optimal transducer for a swept sinusoidal input can be found in the same manner as the double sinusoid. By looking at the energy balance in eq. [4] the energy generated can be described as
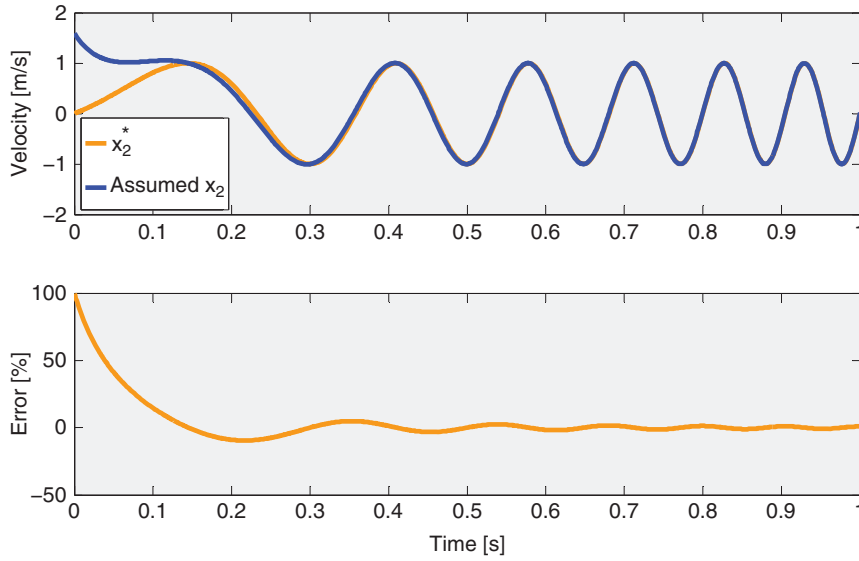
Figure 7: (Top) Velocity trajectories for the assumed optimal (x_2) and actual optimal $(x_2^\star)$ versus time for $A = 1, m = 1, b_m = 1, f_0 = 1, f_r = 10$. (Bottom) The percentage error between the two signals in time. The error quickly decays to zero as the amplitude of the transient decays.

$$
\begin{aligned}
E_{\text{gen}} &= \int_0^t \left[F(t) x_2^\star - b_m x_2^{\star 2} \right] d\tau \\
&= \frac{A^2 m^2 \left(2\sqrt{f_r} t + \text{Cos}\left[\frac{2f_0^2 \pi}{f_r}\right] \left(\text{C}\left[\frac{2f_0}{\sqrt{f_r}}\right] - \text{C}\left[\frac{2(f_0 + f_r t)}{\sqrt{f_r}}\right] \right) + \left(\text{S}\left[\frac{2f_0}{\sqrt{f_r}}\right] - \text{S}\left[\frac{2(f_0 + f_r t)}{\sqrt{f_r}}\right] \right) \text{Sin}\left[\frac{2f_0^2 \pi}{f_r}\right] \right)}{16 b_m \sqrt{f_r}}
\end{aligned}
\tag{53}
$$

where $C[\ ]$ and $S[\ ]$ represent the Fresnel integrals defined as $C[v] = \int_0^v \text{Cos}\left[\frac{\pi t^2}{2}\right] dt$ and $S[v] = \int_0^v \text{Sin}\left[\frac{\pi t^2}{2}\right] dt$, respectively. Noting the boundedness of $C[\ ]$ and $S[\ ]$ an approximation of the energy generated over large periods of time can be expressed as

$$
E_{\text{gen}} \cong \frac{A^2 m^2}{8 b_m} t
\tag{54}
$$

This approximation converges more quickly in time for large values of the ratio $\frac{2f_0}{\sqrt{f_r}}$. That is to say this approximation is more accurate for slow changes in the input frequency relative to the starting frequency. For relatively large time intervals the bounded components of the energy are insignificant compared to the time-dependent components.

The average power output can then be expressed as

$$
P_{\text{RMS}} = \frac{dE_{\text{gen}}}{dt} = \frac{A^2 m^2}{8 b_m}
\tag{55}
$$

This power output is identical to the power output found for a linear system harvesting from a single sinusoid. It is expressed using the damping coefficient, b_m, rather than the damping ratio, ζ_m, and therefore is not an explicit function of frequency.

4 Conclusions

This paper has outlined a framework necessary to relate the form of an input vibration to an optimal transducer force. In creating this framework no assumptions of the transducer architecture were made. This framework was then applied to three case studies. The first was a vibration input of a single sinusoid. The optimal transducer was found to be a linear viscous damper with matched impedance, and a linear spring, resonant to the input frequency. This solution can be expressed as a function of the system states and so is considered a passive system. While the solution of this case study seems trivial, it

demonstrates the method and validates it against a known solution.

The second application was an input consisting of the sum of two sinusoids at different frequencies. The optimal transducer force found was dependent on the difference between the two frequencies. In all cases the optimal transducer force consists of a linear viscous damper with matched impedance, a linear spring, and a time-dependent component. This time-dependent component was found to act as a conservative force, like a time-dependent spring. The framework was used to find the upper limit for power generation. This limit was found to be twice the power output of a linear system harvesting only from the lower of the two frequency components.

The final application was for a swept sinusoidal input. In this case, the optimal transducer contained two portions, a linear viscous damper and a time-dependent component. Here an assumed solution, based on the optimal solution for a stationary sinusoid, was checked against the optimal solution of the framework. It was found that the assumed solution quickly converged to the optimal solution. This case study demonstrates another methodological procedure in which the framework can be used. Specifically, one can assume a solution and then check its performance against the globally optimal solution.

This basic framework could be applied to vibration inputs of various forms to determine the upper bound of power generation for that type of vibration, and the optimal transducer architecture. If a transducer architecture is assumed, a Duffing oscillator for example, this methodology can be applied to determine how close the assumed solution is to the upper bound.

References

Bryson, A. E. 1975. *Applied Optimal Control: Optimization, Estimation and Control*. Boca Raton, Florida: CRC Press Inc.

Daqaq, M. F. 2010. "Response of Uni-Modal Duffing-Type Harvesters to Random Forced Excitations." *Journal of Sound and Vibration* 329 (18): 3621–31. doi:10.1016/j.jsv.2010.04.002

Daqaq, M. F. 2011. "Transduction of a Bistable Inductive Generator Driven by White and Exponentially Correlated Gaussian Noise." *Journal of Sound and Vibration* 330 (11): 2554–64. doi:10.1016/j.jsv.2010.12.005

Daqaq, M. F. 2012. "On Intentional Introduction of Stiffness Nonlinearities for Energy Harvesting under White Gaussian Excitations." *Nonlinear Dynamics* 69 (3): 1063–79. doi:10.1007/s11071-012-0327-0

Daqaq, M., R. Masana, A. Erturk, and D. D. Quinn. 2014. "On the Role of Nonlinearities in Vibratory Energy Harvesting: A Critical Review and Discussion." *Applied Mechanics Reviews* 66: 040801–1–040801–23. doi:10.1115/1.4026278

Erturk, A., J. Hoffmann, and D. J. Inman. 2009. "A Piezomagnetoelastic Structure for Broadband Vibration Energy Harvesting." *Applied Physics Letters* 94 (25): 254102. doi:10.1063/1.3159815

Halvorsen, E. 2008. "Energy Harvesters Driven by Broadband Random Vibrations." *Journal of Microelectromechanical Systems* 17 (5): 1061–71. doi:10.1109/JMEMS.2008.928709

Halvorsen, E. 2013. "Fundamental Issues in Nonlinear Wideband-Vibration Energy Harvesting." *Physical Review E* 87 (4): 042129. doi:10.1103/PhysRevE.87.042129

Halvorsen, E., C. P. Le, P. D. Mitcheson, and E. M. Yeatman. 2013. "Architecture-Independent Power Bound for Vibration Energy Harvesters." *Journal of Physics: Conference Series* 476: 012026. doi:10.1088/1742-6596/476/1/012026

Hoffmann, D., B. Folkmer, and Y. Manoli. 2012. Comparative study of concepts for increasing the bandwidth of vibration based energy harvesters. *Proceedings of PowerMEMS 2012*, 219–222.

Mann, B. P., D. A. Barton, and B. A. Owens. 2012. "Uncertainty in Performance for Linear and Nonlinear Energy Harvesting Strategies." *Journal of Intelligent Material Systems and Structures* 23 (13): 1451–60. doi:10.1177/1045389X12439639.

Mitcheson, P. D., T. C. Green, E. M. Yeatman, and A. S. Holmes. 2004. "Architectures for Vibration-Driven Micropower Generators." *Journal of Microelectromechanical Systems* 13 (3): 1–12.

Nguyen, S. D., E. Halvorsen, and I. Paprotny. 2013. "Bistable Springs for Wideband Microelectromechanical Energy Harvesters." *Applied Physics Letters* 102 (2): 023904. doi:10.1063/1.4775687.

Roundy, S., E. S. Leland, J. Baker, E. Carleton, E. Reilly, E. Lai, B. Otis,, J. M. Rabaey P. K. Wright, and V. Sundararajan. 2005. "Improving Power Output for Vibration-Based Energy Scavengers." *IEEE Pervasive Computing* 4 (1): 28–36. doi:10.1109/MPRV.2005.14

Roundy, S., P. K. Wright, and J. Rabaey. 2003. "A Study of Low Level Vibrations as a Power Source for Wireless Sensor Nodes." *Computer Communications* 26 (11): 1131–44. doi:10.1016/S0140-3664(02)00248-7.